Note: This is the final draft of the subject paper, which was submitted to the ASCE *Practice Periodical on Structural Design and Construction* for final copy-edit and typesetting. The published version of the paper can be found online at https://doi.org/10.1061/(ASCE)SC.1943-5576.0000567.

NEW FORMULATIONS OF BOUSSINESQ SOLUTION FOR VERTICAL AND LATERAL STRESSES IN SOIL

Glenn R. Frazee, P.E.[1]

[1]Sargent & Lundy; Chicago, IL. Email: glenn.r.frazee@sargentlundy.com

Abstract

Calculation of stresses within a soil body due to surface loading is a required step when designing buried commodities and subgrade wall structures. The Boussinesq equation is commonly used for determining stresses in soil due to surface loading, with examples for use found industry-wide. However, the available formulations have limitations, or they only cover simple cases. The purpose of this work is to review the derivation of the Boussinesq equation for vertical and lateral stresses in a soil body and to present several new, closed-form solutions for various surface load cases, including finite line and finite area loads. The formulations are presented as functions of Cartesian coordinates such that the stress at any point in the subsurface plane of interest can be found, not just the peak stress or the stress contour at a specific line. This is particularly useful when considering load distribution at a lateral extent from a finite loading, which may be significantly lower than the peak loading.

INTRODUCTION

Background

Elastician Joseph M. Boussinesq (1885) solved the problem of stress distribution within an elastic, isotropic, infinite half-space when considering a point load at its planar surface in the 1880s. In 1920, it was apparently first proposed by John H. Griffith of Iowa State College that the Boussinesq theory could be applied to the field of soil mechanics (U.S. Bureau of Standards

1920). Since then, many studies (Feld (1923), Gerber (1929), Newmark (1935), Spangler (1938), Haegler (1954), James and Brown (1987), and Rehnman and Broms (1972), for example) have been performed to investigate the applicability of the Boussinesq theory for determining the stress distribution in soils due to surface loading or due to footing pressures. Soil, being an inelastic and anisotropic material, does not behave as perfectly as assumed by the Boussinesq theory, so experimenters have suggested a number of modifications to the basic formulations (see Spangler (1938), Haegler (1954), Terzaghi (1954), James and Brown (1987), and Abdel-Karim (1990)).

This paper reviews the Boussinesq theory and its derivations with respect to its use in the current practice of soil mechanics. It expands upon and is inspired by the work of Newmark (1935) and Marohl (2014), among others. The origins of known formulations are reviewed, and new derivations for special cases are presented. To the author's knowledge, the formulations presented in Appendix I of this paper have not been previously published.

Given the universal use of computers in modern engineering practice, having a programmable methodology for subsurface load determination will lead to efficiency in design. For finite loading, the consideration of subsurface stress distribution at a lateral extent from the load location can be used to reduce the total loading on a buried commodity. This article aims to provide such a methodology for commonly-encountered surface loading types.

To begin, the theoretical basis for the vertical and lateral stresses in a semi-infinite elastic body is reviewed.

Vertical Stress Due to Concentrated Surface Load

As determined by Boussinesq (1885) in the third formula of Equation 83*bis*, the vertical stress due to an elementary load on the surface of an elastic, homogenous, isotropic half-space is given as

$$p_z = \frac{3d\mathrm{P}}{2\pi}\frac{z^2}{r^4}\frac{z}{r}$$

where $d\mathrm{P}$ is the elementary load, z is the vertical distance from the surface to the datum point where the stress is found, $r = \sqrt{x^2 + y^2 + z^2}$, and the xy-plane defines the soil surface. To convert to terms commonly used in today's literature, substitute the point load Q for dP, q_v for p_z, and R for r. Figure 1 illustrates the coordinate system and the variables used. Thus, Boussinesq's Equation 83*bis* is rewritten as

$$q_v(x, y) = \frac{3Q}{2\pi}\frac{z^3}{R^5} = \frac{3Qz^3}{2\pi}\left(x^2 + y^2 + z^2\right)^{-\frac{5}{2}} \tag{1}$$

Since (1) is written in terms of x, y, and z, it is readily suitable for programming into a computer.

A typical contour plot of the vertical stresses due to a concentrated surface load is displayed in Figure 2. This plot uses a 10-kN point load and shows the load contour at a depth of 1 m. Note the bell shape typical of the vertical stresses determined using this method.

The indefinite integral of (1) has the form shown in (2), given by Newmark (1935) and independently verified by the author. After integrating with respect to x, point load Q is replaced by line load p.

$$\frac{3Qz^3}{2\pi}\int\left(x^2 + y^2 + z^2\right)^{-\frac{5}{2}} dx = \frac{pz^3}{2\pi}\left[\frac{x\left[2x^2 + 3(y^2 + z^2)\right]}{(y^2 + z^2)^2\ (x^2 + y^2 + z^2)^{\frac{3}{2}}}\right] \tag{2}$$

Integrating (2) with respect to y, the author finds (replacing line load p with area load q)

$$\frac{pz^3}{2\pi}\int \frac{x\left[2x^2 + 3(y^2 + z^2)\right]}{(y^2 + z^2)^2\ (x^2 + y^2 + z^2)^{\frac{3}{2}}}\, dy = \frac{q}{2\pi}\left[\frac{xyz(x^2 + y^2 + 2z^2)}{(x^2 + z^2)(y^2 + z^2)\sqrt{x^2 + y^2 + z^2}} + \tan^{-1}\left(\frac{xy}{z\sqrt{x^2 + y^2 + z^2}}\right)\right] \tag{3}$$

the second part of which (inside the inverse tangent) does not exactly match that determined by Newmark (1935). However, verification by differentiation shows this integral to also be valid, and it is slightly simpler than Newmark's.

Radial Stress Due to Concentrated Surface Load

Boussinesq (1885), on pages 106-107, notes that (translated from French)

> ...by means of formulas (81) or (43), the circular conaxial cylinders described around the z-axis or the force dP undergo, per unit area, *compressions* (positive or negative)

whose normal component is

$$\frac{dP}{2\pi r^2}\left[3\frac{z}{r}\left(1-\frac{z^2}{r^2}\right)-\frac{\mu}{\lambda+\mu}\frac{r}{r+z}\right] \tag{4}$$

Again substitute the point load Q for dP and R for r. The coefficients μ and λ are known as *Lamé's Constants*, and according to Timoshenko and Goodier (1970) have the values

$$\mu = \frac{E}{2(1+\nu)} \qquad \lambda = \frac{\nu E}{(1+\nu)(1-2\nu)}$$

where E is the modulus of elasticity and ν is Poisson's ratio of the material. Substituting these into (4) and rearranging, one finds that the radial stress q_r (the "normal component" identified by Boussinesq above) is

$$q_r = \frac{Q}{2\pi R^2}\left[\frac{3r^2 z}{R^3}-\frac{(1-2\nu)R}{R+z}\right] \tag{5}$$

Note that this equation is written using polar coordinates and it considers the stress at a certain radial distance R from the point load, with the stress component applied along the radius. When considering the lateral stress on a flat wall at distance x from a point load as in Figure 3, (5) can be adjusted as such:

$$q_x(y,z) = \frac{\psi Q}{2\pi}\left[\frac{3x^2 z}{(x^2+y^2+z^2)^{\frac{5}{2}}}-\frac{1-2\nu}{(x^2+y^2+z^2)+z\sqrt{x^2+y^2+z^2}}\right] \tag{6}$$

See discussion in the next section for factor ψ. Note that often (6) is further simplified by considering that Poisson's ratio for the material is 0.50 (i.e., the material is incompressible). This assumption is sufficient, and conservative, for most purposes in evaluating the lateral stress transmitted through soil (see Figure 4), and is commonly used in industry standards, such as AASHTO (2017). As shown in Figure 4, Poisson's ratios less than 0.50 not only result in reduced lateral stresses, but they also predict tensile stresses in portions of the soil.

Figure 5 displays a typical contour plot of the lateral stress due to a concentrated surface load. A 40-kN load is considered at 1 m distance from the vertical wall surface, and Poisson's ratio is taken as 0.50.

The first indefinite integral of (6) with respect to y is shown below in (7).

$$\frac{\psi p}{2\pi x}\left[\frac{x^3yz(3x^2+2y^2+3z^2)}{(x^2+z^2)^2(x^2+y^2+z^2)^{\frac{3}{2}}}-(1-2\nu)\left[\tan^{-1}\left(\frac{y}{x}\right)-\tan^{-1}\left(\frac{yz}{x\sqrt{x^2+y^2+z^2}}\right)\right]\right] \tag{7}$$

Equation 6 can also be integrated instead with respect to x, as in (8).

$$\frac{\psi p}{2\pi}\left[\frac{x^3z}{(y^2+z^2)(x^2+y^2+z^2)^{\frac{3}{2}}}-\frac{(1-2\nu)}{y}\left[\tan^{-1}\left(\frac{x}{y}\right)-\tan^{-1}\left(\frac{xz}{y\sqrt{x^2+y^2+z^2}}\right)\right]\right] \tag{8}$$

In practice, the second part of (8) that is multiplied by $(1-2\nu)/y$ is problematic since it cannot be evaluated at $y=0$. For this case, consider the limit as y approaches zero:

$$\lim_{y\to 0}\ \frac{1}{y}\left[\tan^{-1}\left(\frac{x}{y}\right)-\tan^{-1}\left(\frac{xz}{y\sqrt{x^2+y^2+z^2}}\right)\right]=\frac{\sqrt{x^2+y^2}-z}{xz} \tag{9}$$

Therefore, re-write (8) as

$$\frac{\psi p}{2\pi}\left[\frac{x^3z}{(y^2+z^2)(x^2+y^2+z^2)^{\frac{3}{2}}}\right.$$
$$\left.-(1-2\nu)\begin{cases}\dfrac{\sqrt{x^2+y^2}-z}{xz} & \text{if } y=0\\[2ex] \dfrac{1}{y}\left[\tan^{-1}\left(\dfrac{x}{y}\right)-\tan^{-1}\left(\dfrac{xz}{y\sqrt{x^2+y^2+z^2}}\right)\right] & \text{otherwise}\end{cases}\right] \tag{10}$$

For further integration of (7) in terms of x or of (8) in terms of y, the portion of the equation that is multiplied by $(1-2\nu)$ does not integrate cleanly. Therefore, Poisson's ratio is assumed to be equal to 0.50, and this portion of the equation simplifies to zero. Thus, the partial indefinite double integral of (6) is found below in (11).

$$\frac{\psi q}{2\pi}\left[\tan^{-1}\left(\frac{xy}{z\sqrt{x^2+y^2+z^2}}\right)-\frac{xyz}{(x^2+z^2)\sqrt{x^2+y^2+z^2}}\right] \tag{11}$$

Rigid vs. Yielding Walls

Research by Spangler (1938) suggests that for subgrade walls with a high degree of rigidity, the interrupting effect of the wall effectively increases the lateral stress resisted by the wall beyond that which would be predicted by a purely elastic solution. The author has chosen to represent this effect with symbol ψ herein. Spangler and AASHTO consider a factor of $\psi = 2$ for rigid walls.

Unless justification can be provided to consider the wall non-rigid, ψ should conservatively be taken as 2 in all cases. See further discussion in AASHTO (2017), Section 3.11.

NEW STRESS FORMULATIONS

Considering the equations determined in (2), (3), (7), (8), and (11), it is possible to develop closed-form solutions to the Boussinesq problem for different load patterns, the derivations of which are available in Appendix II. Certain formulations, especially those for infinite loading, have been available in the literature for some time (see Poulos and Davis (1991) for example). It should also be noted that solutions for finite area loading have also been available; however, these have limitations. For example, Newmark (1935) and Gray (1936) provide means of finding the vertical stress under the corner of a finite rectangular area, which one can extrapolate to find the loading at any point under the rectangle by considering rectangular areas of different sizes. This is, however, a time-consuming process, and it makes determining the vertical stress contour on the subgrade very tedious.

Review of the literature also shows that Poisson's ratio is typically assumed equal to 0.50 when developing the formulations for lateral stress. As noted by AASHTO (2017), Poisson's ratio for soil can vary from about 0.25 (granular and stiff cohesive soils) to 0.49 (soft cohesive soils), and as such, load reductions can be realised if the soil properties are known. Where appropriate, these lateral stress solutions are presented anew, this time with Poisson's ratio of the soil considered in the formulation.

As far as the author can tell, closed-form solutions for subsurface stresses at any point due to finite line and finite area loads are not available and are therefore presented for the first time herein. Figures 10 to 17 in Appendix I present the new formulations for vertical and lateral stress in soil due to different load types. These are presented as functions of Cartesian coordinates and are relatively easy to program into even simple computer software.

DESIGN PROCEDURE

To find the stress contour for a subsurface commodity using the formulations contained in Appendix I, consider the following process:

1. Categorize surface loads based on load type (point, line, area, etc.).
2. Determine locations of loaded areas and assign coordinates using a Cartesian grid. Locations should all be consistent with an established coordinate origin; see Figures 10 to 17 for coordinate system.
3. Assign discrete functions for each loading (eg. $f_1(x, y)$ for the first load, $f_2(x, y)$ for the second, etc.).
4. Combine the contributions of each load using superposition ($f_{comb} = \sum_1^n f_n(x, y)$).
5. A graph of the combined stress contour can be plotted, if desired (similar to Figure 6). This provides a good check that the formulations are entered correctly.
6. If the location of the subsurface commodity is known relative to the different surface loads, the relative location can be used to determine the maximum stress at the commodity location. Alternatively, in the case of a load moving over a stationary commodity, the peak stress for the entire plot can be found.
7. Further load reduction can be realized by integrating the combined stress contour over the effective width and length of the commodity and averaging, which is especially beneficial when acute peaks are observed in the contour (see Marohl (2014)).

DESIGN EXAMPLE

For a sample problem, consider the crawler crane setup shown in Figure 7. Spreader mats are used to reduce the bearing pressures under the tracks to an acceptable value. The crane spreader mats are set up 2 m from the exterior rigid subgrade wall of a building, and the vertical bearing pressure from the spreader mats will induce lateral stresses on the wall. Figure 7 shows the bearing pressures under the mats, and for this particular lift the rightmost mat sees a higher bearing pressure. The critical variables are summarized in Table 1.

Prior to the finite area loading formulation presented in Figure 17, the best way to approximate this load pattern using the available literature may have been to use the formulation for an infinite strip load. Using the formulations in Figure 17 and the method of superposition, one can combine the results for the left and right spreader mats and determine the plot of the lateral stress on the subgrade wall, as in Figure 8. By approximating the spreader mats as an infinite strip load of 150 kPa, width of 5 m, at a distance of 2 m from the wall, the resulting lateral stress is much larger, as in Figure 9. For comparison, the plot of the lateral stress due to the finite area loads at $y = 2.365$ m, which is the line of maximum stress in Figure 8, is also included in Figure 9. The author has entered the finite area and infinite strip formulations into a calculation package to determine the maxima of the functions. These are approximately 27 kPa (finite area loads) and 71 kPa (infinite strip load), so use of the finite area formulation results in a reduction in maximum lateral stress of 62%.

CONCLUSIONS

Presented herein is a discussion on the historical basis of the use of the Boussinesq formula for determining the vertical and lateral stresses in a soil mass. Included in Appendix I also are new closed-form solutions for different surface load patterns using the Boussinesq equations. Since they use simple algebraic and trigonometric functions, these closed-form solutions are useful for computer programming packages lacking advanced numeric integration capabilities.

Depending on the exact configuration of the surface loads, consideration of finite loading patterns can lead to significantly lower subgrade stresses as compared to approximation using infinite loading patterns, thereby reducing material costs in the design phase. Alternatively, for re-evaluation of existing structures and subsurface commodities, refinement in applied loading can reduce or remove the requirement for costly reinforcement.

As shown in Appendix I, some of the developed closed-form equations can be lengthy and cumbersome. Assuming that more advanced software packages are available to the user that have the capability, it may be more concise to perform the numeric integration directly from (1) and (6) in lieu of using the closed-form solutions.

APPENDIX I: NEW STRESS FORMULATIONS

This Appendix contains the new closed-form solutions of the Boussinesq equations for vertical and lateral stress in soil due to different load types. Presented in Figures 10 to 17 are the load pattern and example subgrade stress distribution for the load type, along with the correlating formulations developed by the author.

APPENDIX II: FORMULA DERIVATION AND VALIDATION

Vertical Stress Due to Finite Line Load

Consider a finite line load starting at $x = a$ and ending at $x = b$, parallel to the x-axis, located at $y = c$, as depicted in Figure 10. In this case, to determine the formulation for the vertical stress at depth z at any coordinate (x, y), the integral evaluated in (2) is adjusted as shown in (12).

$$q_v(x, y) = \frac{3pz^3}{2\pi} \int_{a-x}^{b-x} \left[m^2 + (c - y)^2 + z^2\right]^{-\frac{5}{2}} dm \tag{12}$$

Following (2), evaluation of this integral results in the equation for the vertical stress due to a finite line load shown in Figure 10. To validate, compare the results of (12) to that of the infinite line loading formulation in Poulos and Davis (1991):

$$q_v(y) = \frac{2p}{\pi} \frac{z^2}{(y^2 + z^2)^2}$$

Consider a 10-kN/m line load distributed over 1-m, 5-m, and infinite extents, with the vertical stress found at a depth of 2 m below the midpoint of the line load. The stress contours for these conditions are displayed in Figure 18. As the length of the line load relative to the depth increases, the vertical stress approaches that found for an infinite line load. Therfore, the results of (12) are consistent with the infinite line load formulation, and the new formulation in Figure 10 is valid.

Lateral Stress Due to Finite Line Load Parallel to Wall

Consider a finite line load starting at $y = c$ and ending at $y = d$, parallel to the wall face, located at $x = a$, as depicted in Figure 11. In this case, to determine the formulation for the lateral stress at any coordinate (y, z), integrate (6) as shown in (13).

$$q_x(y,z) = \frac{\psi p}{2\pi} \int_{c-y}^{d-y} \left[\frac{3a^2 z}{\left[a^2+n^2+z^2\right]^{\frac{5}{2}}} - \frac{1-2\nu}{\left[a^2+n^2+z^2\right] + z\sqrt{a^2+n^2+z^2}} \right] dn \tag{13}$$

Following (7), evaluation of the integral in (13) results in a lengthy equation, which is broken into parts f_a and f_b for ease of use (see Figure 11). Part f_b is multiplied by a term containing Poisson's ratio and, as noted previously, can be omitted if one assumes $\nu = 0.50$.

For validation, consider a 70-kN/m line load, 2 m from the wall face, distributed over 6-m and 10-m extents with Poisson's ratio taken as 0.40 and 0.50, respectively, in two separate cases. Also consider an infinite line loading of the same magnitude and at the same distance from the wall, using the following equation per Poulos and Davis (1991), which does not include the effect of Poisson's ratio:

$$q_x(z) = \frac{2p}{\pi} \frac{x^2 z}{(x^2+z^2)^2}$$

Value ψ is taken as 1. The stress contours for these conditions are displayed in Figure 19. Similar to the previous section, as the length of the line load relative to the distance from the wall increases and as ν approaches 0.50, the lateral stress converges on that found for an infinite line load, thereby validating the new formulation in Figure 11.

Lateral Stress Due to Finite Line Load Perpendicular to Wall

Consider a finite line load starting at $x = a$ and ending at $x = b$, perpendicular to the wall face, located at $y = c$, as depicted in Figure 12. In this case, to determine the formulation for the lateral stress at any coordinate (y, z), integrate (6) as shown in (14).

$$q_x(y,z) = \frac{\psi Q}{2\pi} \int_a^b \left[\frac{3x^2 z}{\left[x^2 + (c-y)^2 + z^2\right]^{\frac{5}{2}}} - \frac{1-2\nu}{\left[x^2 + (c-y)^2 + z^2\right] + z\sqrt{x^2 + (c-y)^2 + z^2}} \right] dx \quad (14)$$

Integration follows (10), which results in a lengthy equation that is split into parts f_a and f_b (see Figure 12). Part f_b is multiplied by a term containing Poisson's ratio and can be omitted if one assumes $\nu = 0.50$.

It can be shown by rearranging (14) that the formulation for the lateral stress contour at $y = c$ matches that given in AASHTO (2017), so this formulation is valid by comparison. However, for $y \neq c$, the formulation must be validated. Consider a short line load of 1000 kN/m, 0.1 m long, located 1 m from the wall face ($a = 1$ m, $b = 1.1$ m). Two cases are run, one with $\nu = 0.40$ and the other with $\nu = 0.50$. For comparison, use a 100 kN point load per (6), also located 1 m from the wall and with $\nu = 0.50$, and also assume that both loads are located at $y = 0$ and that $\psi = 2$. The lateral stress contour is found at $y = 0.5$ m in order to validate the formulation in Figure 12. Figure 20 displays the stress contours for these cases. In the author's testing, if the point load is located 1.05 m from the wall (centered on the finite line load), the curves for the point load and the finite line load with $\nu = 0.50$ overlap.

Lateral Stress Due to Infinite Line Load Parallel to Wall

Figure 13 displays an infinite line load parallel to a vertical wall surface, located at $x = a$. The lateral stress is found by integrating (6) and evaluating at infinite extents:

$$q_x(y,z) = \frac{\psi p}{2\pi} \int_{-\infty}^{\infty} \left[\frac{3a^2 z}{\left[a^2 + y^2 + z^2\right]^{\frac{5}{2}}} - \frac{1-2\nu}{\left[a^2 + y^2 + z^2\right] + z\sqrt{a^2 + y^2 + z^2}} \right] dy \quad (15)$$

This is accomplished by considering the indefinite integral in (7) and taking the limits as $y \to \infty$ and $y \to -\infty$, which results in the equation in Figure 13. The first part of this equation has been known in the literature for some time (see Poulos and Davis (1991)); however, the portion containing Poisson's ratio appears to be shown for the first time herein.

For validation, consider a 70-kN/m line load, 2 m from the wall face, with Poisson's ratio taken as 0.40 and 0.45, respectively, in two separate cases. Also consider an infinite line loading of the same magnitude and at the same distance, using the equation per Poulos and Davis (1991), which does not include the effect of Poisson's ratio. Value ψ is taken as 1. The stress contours for these conditions are displayed in Figure 21. As expected, the magnitude of the lateral stress increases and the formula developed by the author converges on that from Poulos and Davis as v approaches 0.50.

Vertical Stress Due to Infinite Strip Load

The vertical stress below an infinite strip load is found first by finding the indefinite integral of the vertical stress formula per Poulos and Davis (1991), Eqn. 2.7b. The line load p is replaced by area load q.

$$q_v(y) = \frac{2qz^3}{\pi} \int \left[y^2 + z^2\right]^{-2} dy = \frac{q}{\pi} \left[\tan^{-1}\left(\frac{y}{z}\right) + \frac{yz}{y^2 + z^2}\right] \tag{16}$$

To determine the formula for the infinite strip loading in Figure 14, adjust (16) for the extents of the strip loading as shown below.

$$q_v(y) = \frac{2qz^3}{\pi} \int_{c-y}^{d-y} \left[n^2 + z^2\right]^{-2} dn \tag{17}$$

The result of this intergral is shown in Figure 14 and is valid for any location x along the strip load.

Note that this equation is often given in terms of an angle with respect to the vertical (see Poulos and Davis (1991)), which makes it appear, superficially, more simplified than determined herein. However, this requires additional steps by the user in order to translate the equation into a function of y and z, so the equation in Figure 14 is more readily suited to being programmed into a computer.

To validate the infinite strip formula, consider a 50-kPa strip load distributed over a 1-m width. This is compared to a 50-kN/m line load, which is equivalent to the strip load, just concentrated on a line. For both, the vertical stress found at a depth of 2 m below the strip or the line. The stress contours for these conditions are displayed in Figure 22 and they are nearly identical.

Vertical Stress Due to Finite Area Load

Consider a finite area load extending between $x = a$ and $x = b$ and between $y = c$ and $y = d$, as depicted in Figure 15. In this case, the vertical stress at depth z at any coordinate (x, y) is found by taking the double integral of (1), adjusted to substitute area load q for point load Q, as shown in (18).

$$q(x, y) = \frac{3qz^3}{2\pi} \int_{c-y}^{d-y} \int_{a-x}^{b-x} \left[m^2 + n^2 + z^2\right]^{-\frac{5}{2}} dm\, dn \tag{18}$$

Evaluation of the integral in (18) results in a lengthy equation for the vertical stress due to a finite area load. Since there are four parts of the equation that follow the same pattern as in (3), a generic function for these parts is developed:

$$f(\beta, \delta) = \frac{z(\beta - x)(\delta - y)[(\beta - x)^2 + (\delta - y)^2 + 2z^2]}{[(\beta - x)^2 + z^2][(\delta - y)^2 + z^2]\sqrt{(\beta - x)^2 + (\delta - y)^2 + z^2}} + \tan^{-1}\left[\frac{(\beta - x)(\delta - y)}{z\sqrt{(\beta - x)^2 + (\delta - y)^2 + z^2}}\right] \tag{19}$$

The vertical stress at depth z and coordinate (x, y) can then be found as shown in Figure 15, with the values a, b, c, and d replacing β and δ as indicated.

To validate the finite area formula, consider a 50-kPa area load distributed over a 1-m width and over lengths of 3 m and 6 m. This is compared to a 50-kPa infinite strip load, also of 1-m width. The vertical stress is found at a depth of 2 m below the surface, and the stress contour is centered on the midpoint of the area or the strip. The stress contours for these conditions are displayed in Figure 23. As the finite rectangular area elongates, the vertical stress contour converges to that of the infinite strip, as expected, thereby validating the formulations in Figure 15.

Lateral Stress Due to Infinite Strip Load Parallel to Wall

Figure 16 displays an infinite strip load parallel to a wall face. To find the equation for this case, start with the equation for for an infinite line load parallel to the wall face in Figure 13, replacing the line load p with area load q, and integrating from $x = a$ to $x = b$. As before in (11), the portion of the formula containing Poisson's ratio is dropped assuming that $\nu = 0.50$.

$$q_x(z) = \frac{2\psi q z}{\pi} \int_a^b \frac{x^2}{(x^2+z^2)^2}\, dx = \frac{q}{\pi}\left[\frac{az}{a^2+z^2} - \frac{bz}{b^2+z^2} + \tan^{-1}\left(\frac{b}{z}\right) - \tan^{-1}\left(\frac{a}{z}\right)\right] \tag{20}$$

The inverse tangent portions of (20) can be combined using the trigonometric identity

$$\tan^{-1} u - \tan^{-1} v = \tan^{-1}\left(\frac{u-v}{1+uv}\right)$$
$$\tan^{-1}\left(\frac{b}{z}\right) - \tan^{-1}\left(\frac{a}{z}\right) = \tan^{-1}\left(\frac{z(b-a)}{z^2+ab}\right)$$

which has the advantage of removing the divide by zero issues in the equation. Thus, the lateral stress due to an infinite strip load is found per Figure 16.

Similar to the case with the vertical stress due to an infinite strip load, the equation in Figure 16 is typically given in terms of an angle with respect to the wall face (see AASHTO (2017)). However, the equation herein is more fitting for direct entry into a computer programming subroutine.

For validation, consider a thin strip load of 1000 kPa, 0.1 m in width, starting 2 m from the wall face. Also consider an infinite line loading of 100 kN/m (effectively the same magnitude of loading as the infinite strip, just concentrated in a line) located 2 m from the wall, using the equation per Poulos and Davis (1991) given previously. Value ψ is taken as 1. The stress contours for these conditions are displayed in Figure 24. The two lines are nearly identical. In the author's testing, the two lines overlap completely when the infinite line loading is placed 2.05 m away from the wall (i.e., centered on the infinite strip load).

Consider also a special case of this loading where $a = 0$ and b is any positive number. In this case, (20) simplifies to

$$q_x(z) = \frac{\psi q}{\pi}\left[\tan^{-1}\left(\frac{b}{z}\right) - \frac{bz}{b^2+z^2}\right] \tag{21}$$

This formulation also has divide by zero issues at $z = 0$ and must be conditioned. Taking the limit as $z \to 0^+$, the portion of (21)inside the brackets converges to $\pi/2$, and therefore

$$q_x(z) = \begin{cases} \dfrac{\psi q}{2} \text{ if } z = 0 \\ \dfrac{\psi q}{\pi}\left[\tan^{-1}\left(\dfrac{b}{z}\right) - \dfrac{bz}{b^2+z^2}\right] \text{ otherwise} \end{cases} \tag{22}$$

It is also worth noting that when $b \to \infty$, (22) converges to $\psi q/2$ for all depths of z, as one might expect for an infinite, uniform, vertical surcharge load.

Lateral Stress Due to Finite Rectangular Area Load

Consider a finite rectangular vertical pressure extending between $x = a$ and $x = b$ and between $y = c$ and $y = d$, as depicted in Figure 17. In this case, to determine the formulation for the lateral stress at depth z and location y, integrate (6) as shown in (23). Per (11), Poisson's ratio is assumed to be 0.50.

$$q_x = \frac{3\psi q z}{2\pi} \int_{c-y}^{d-y} \int_a^b \frac{x^2}{[x^2+n^2+z^2]^{\frac{5}{2}}} dx\, dn \tag{23}$$

Evaluation of the integral in (23) results in a lengthy equation for the lateral stress due to a finite rectangular area load. Since there are four parts of the equation that follow the same pattern as in (11), a generic function for these parts is developed:

$$f(\beta,\delta) = \tan^{-1}\left[\frac{\beta(\delta-y)}{z\sqrt{\beta^2+(\delta-y)^2+z^2}}\right] - \frac{\beta z(\delta-y)}{[\beta^2+z^2]\sqrt{\beta^2+(\delta-y)^2+z^2}} \tag{24}$$

The lateral stress at depth z and location y can then be found as shown in Figure 17, with the values a, b, c, and d replacing β and δ as indicated.

To validate the finite area formula, consider a 50-kPa area load distributed over a 1-m width and over lengths of 3 m and 6 m ($d = -c = 1.5$ m and 3 m, respectively). This is compared to a 50-kPa infinite strip load, also of 1-m width. All loads are located 2 m from the face of the wall ($a = 2$ m and $b = 3$ m), ψ is taken as 2, and the stress contour is centered on the midpoint of the finite area ($y = 0$). The stress contours for these conditions are displayed in Figure 25. As the finite rectangular area elongates, the lateral stress contour converges to that of the infinite strip, as expected.

DATA AVAILABILITY STATEMENT

No data, models, or code were generated or used during the study.

ACKNOWLEDGMENTS

The author would like to thank his colleague Michael P.H. Marohl, P.E. (Sargent & Lundy) for providing helpful feedback on this paper and continual collaboration on the Boussinesq theory, and also the peer reviewers for reviewing this paper and providing constructive comments.

NOTATION

The following symbols are used in this paper:

a, b	=	distances from the y-axis (m);
c, d	=	distances from the x-axis (m);
p	=	applied line load at soil surface (kN/m);
Q	=	applied point load at soil surface (kN);
q	=	applied area load at soil surface (kPa);
q_v	=	vertical stress in horizontal soil layer (kPa);
q_x	=	lateral stress on subgrade vertical surface (kPa);
$\tan^{-1}$	=	inverse tangent function (result in radians);
x, y, z	=	Cartesian coordinates (m); and
ψ	=	wall rigidity factor (1 for flexible walls, 2 for rigid walls, see discussion).

References

Abdel-Karim, A. M. e. a. (1990). “Live load distribution on concrete box culverts.” *Transportation Research Record 1288*, 136–151.

American Association of State Highway and Transportation Officials (AASHTO) (2017). *LRFD Bridge Design Specifications*. AASHTO, Washington, D.C., 8th edition.

Boussinesq, J. (1885). “Application des potentiels à l’étude de l’équilibre et du mouvement des solides élastiques [Application of potentials to the study of the equilibrium and movement of elastic solids].” *Mémoires de la Société des Sciences, 4e Série, Tome XIII*, 104–107.

Feld, J. (1923). “Lateral earth pressure: The accurate experimental determination of the lateral earth pressure, together with a resume of previous experiments.” *Proc., Am. Soc. of Civil Eng.*, Vol. 49, 1448–1505.

Gerber, E. (1929). *Untersuchungen über die Druckverteilung im örtlich belasteten Sand [Studies on the pressure distribution in locally loaded sand]*. Diss.-Druckerei A.-G. Gebr. Leemann & Co., Zurich.

Gray, H. (1936). “Stress distribution in elastic solids.” *Proc., Intl. Conf. on Soil Mech.*, Vol. 2, 157–162.

Haegler, J. B. (1954). “Horizontal pressures on retaining walls due to line surface loads.” M.S. thesis, The Univ. of Missouri, Rolla, MO.

James, R. W. and Brown, D. E. (1987). “Wheel-load-induced earth pressures on box culverts.” *Transportation Research Record 1129*, 55–62.

Marohl, M. P. H. (2014). “PVP2014-28467: Comparison of numerical methods for calculation of vertical soil pressures on buried piping due to truck loading.” *Proc. ASME 2014 Pressure Vessels & Piping Conf.*, Am. Soc. of Mech. Eng., Anaheim, CA.

Newmark, N. M. (1935). “Simplified computation of vertical pressures in elastic foundations.” *Circular No. 24, Engineering Experiment Station*, University of Illinois Bulletin, Urbana, IL.

Poulos, H. G. and Davis, E. H. (1991). *Elastic Solutions for Soil and Rock Mechanics*. Centre for Geotechnical Research, University of Sydney.

Rehnman, S. E. and Broms, B. B. (1972). “Lateral pressures on basement wall. Results from full-scale tests.” *Fifth Eur. Conf. On Soil Proc.*, 189–197.

Spangler, M. G. (1938). “Horizontal pressures on retaining walls due to concentrated surface loads.” *The Iowa State College Bulletin*, Iowa State College of Agriculture and Mechanic Arts, Ames, IA.

Terzaghi, K. (1954). “Anchored bulkheads.” *Trans., Am. Soc. of Civil Eng.*, Vol. 119, 1243–1280.

Timoshenko, S. P. and Goodier, J. N. (1970). *Theory of Elasticity*. McGraw-Hill, New York, 3rd edition.

U.S. Bureau of Standards (1920). “Revised report of sub-committee on soils.” *Proc., Am. Soc. of Civil Eng.*, Vol. 46, 916–941.

List of Tables

Load ID	Type	q (kPa)	a (m)	b (m)	c (m)	d (m)
1	Finite Area	100	2	7	-3.5	-1.5
2	Finite Area	150	2	7	1.5	3.5

Table 1. Crane Spreader Mat Example Critical Variables

List of Figures

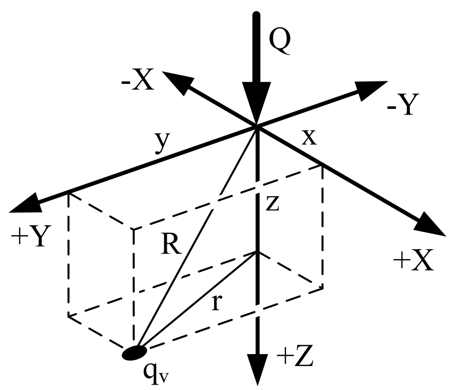

Fig. 1. Coordinate System for Surface Point Load

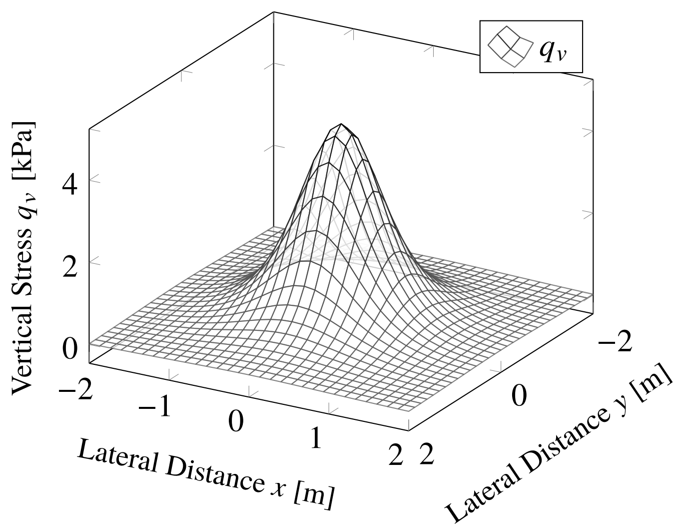

Fig. 2. Vertical Stress Contour Due to Concentrated Surface Load

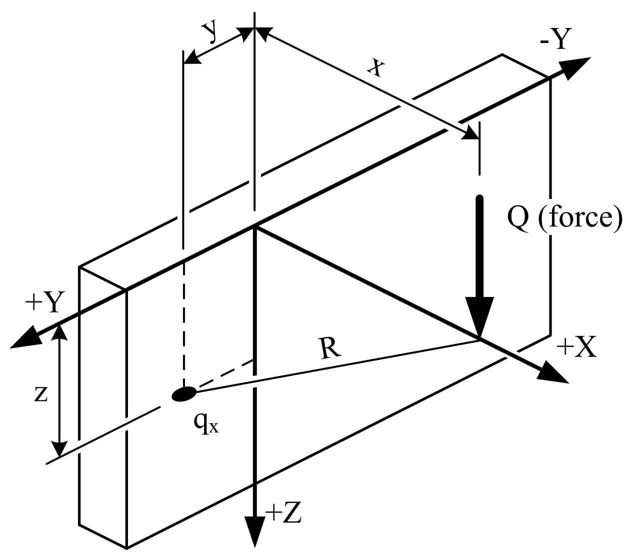

Fig. 3. Concentrated Surface Load Adjacent to Subgrade Wall

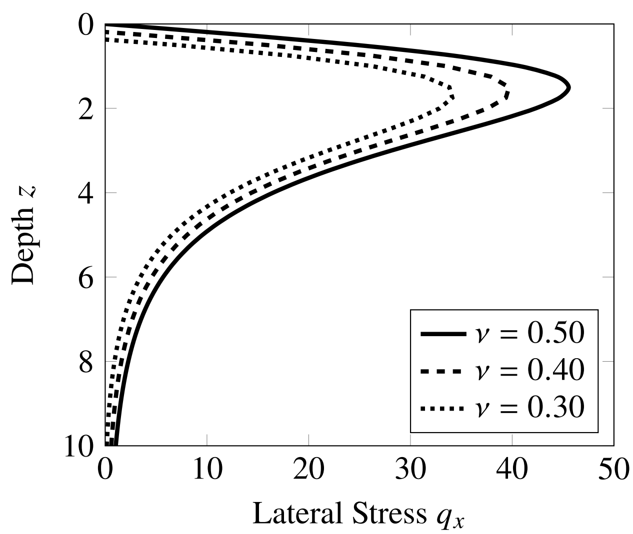

Fig. 4. Effect of Poisson's Ratio ν on Lateral Stress Contour

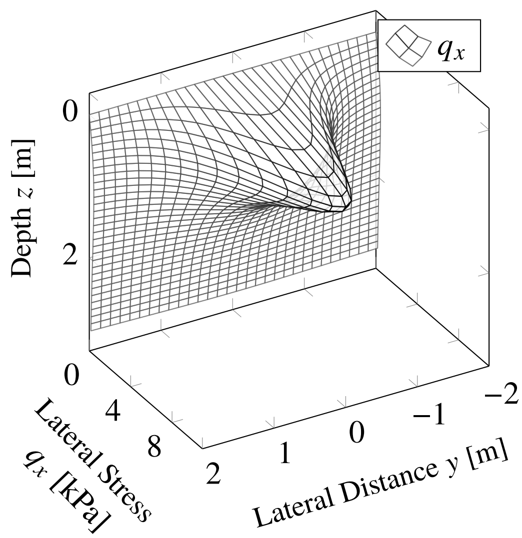

Fig. 5. Lateral Stress Contour Due to Concentrated Surface Load

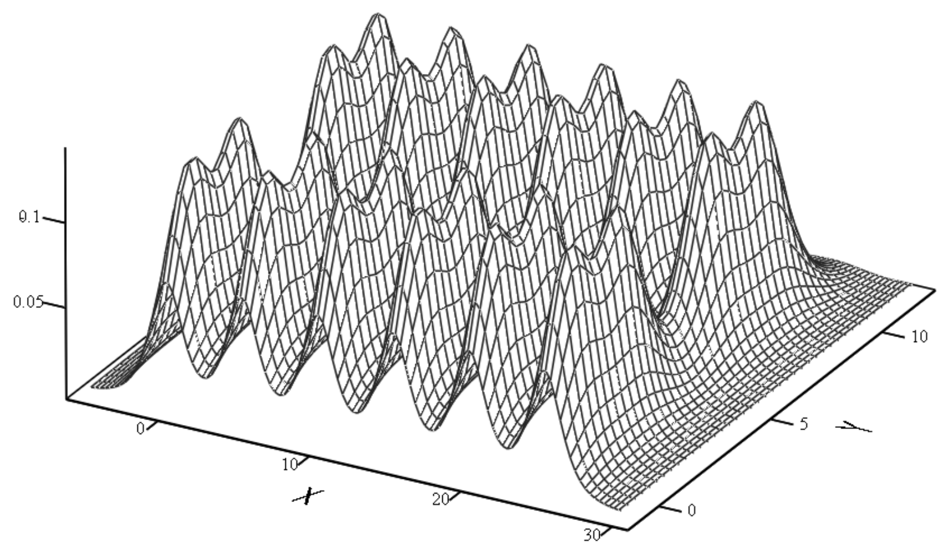

Fig. 6. Example Pressure Contour Using Superposition of Point Load Array

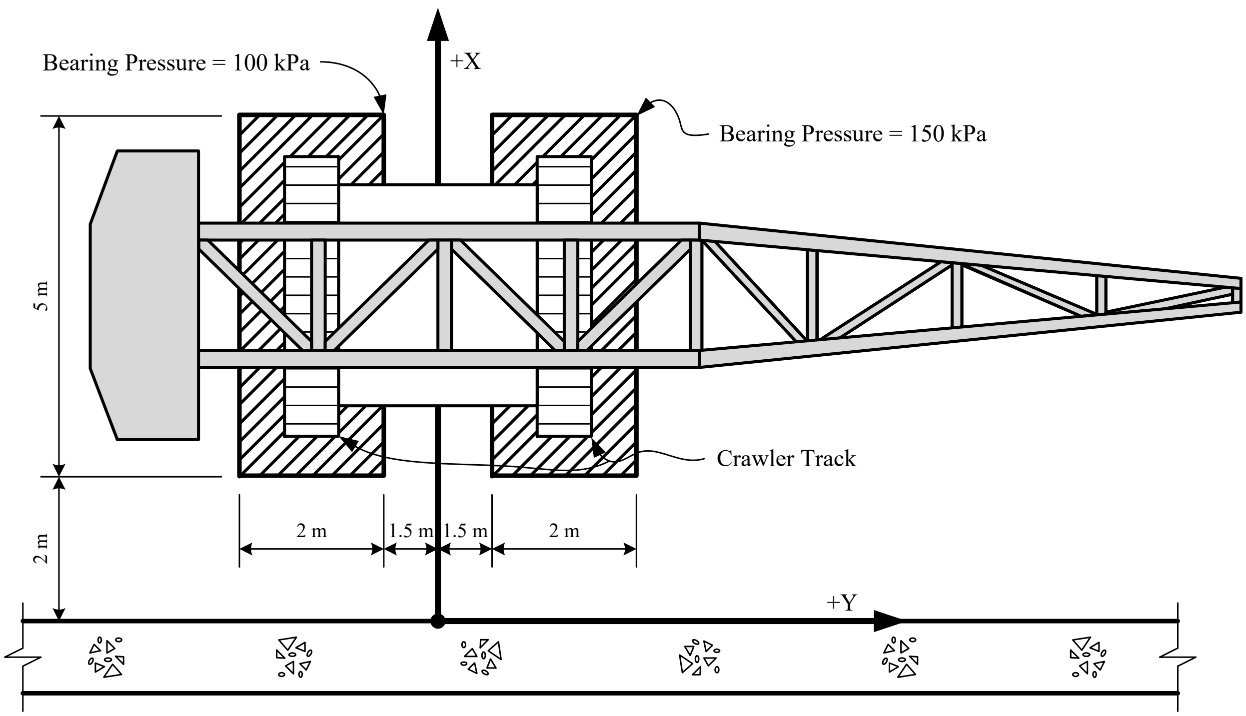

Fig. 7. Crane Spreader Mat Example Problem

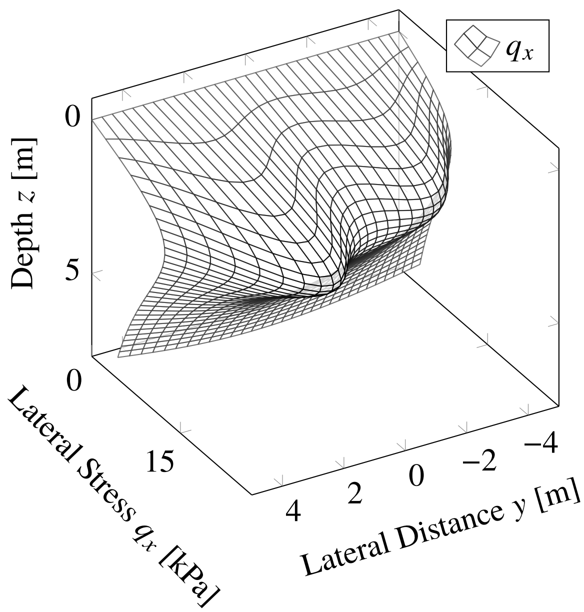

Fig. 8. Lateral Stress Contour Due to Example Crane Loading

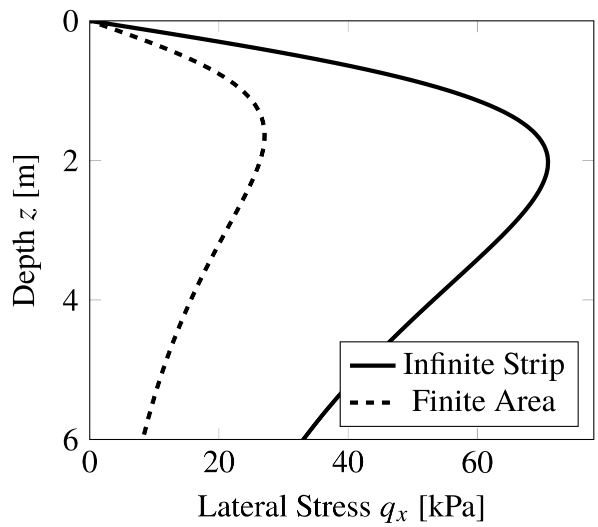

Fig. 9. Comparison of Lateral Stress Contours, Infinite Strip vs. Finite Area

Fig. 10. Vertical Stress Due to Finite Line Load

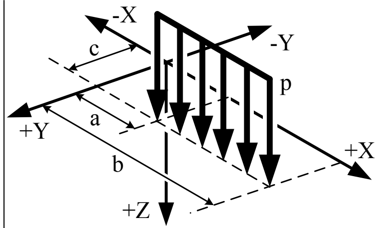

Sample stress distribution generated using the following parameters:
$p = 15$ kN/m
$a = 5$ m
$b = 15$ m
$c = 0$ m
$z = 2$ m

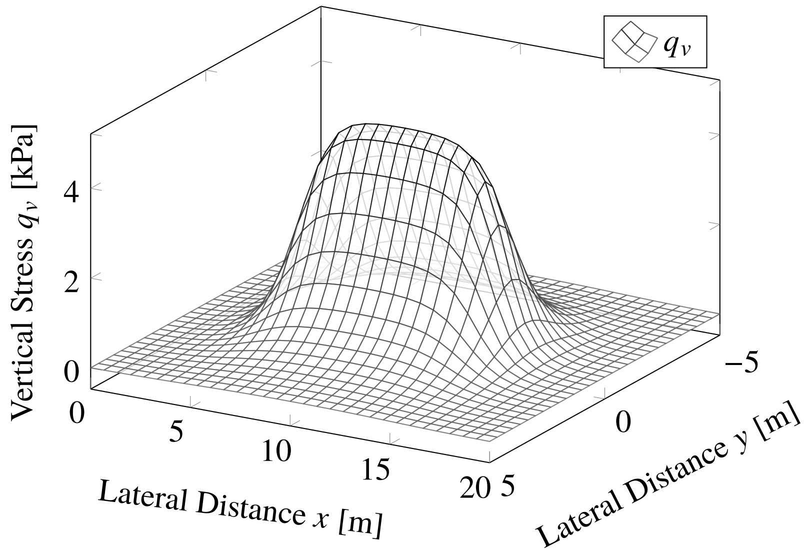

$$q_v(x,y) = \frac{pz^3}{2\pi[(c-y)^2+z^2]^2}\left[\frac{(b-x)\left[2(b-x)^2+3[(c-y)^2+z^2]\right]}{[(b-x)^2+(c-y)^2+z^2]^{\frac{3}{2}}} - \frac{(a-x)\left[2(a-x)^2+3[(c-y)^2+z^2]\right]}{[(a-x)^2+(c-y)^2+z^2]^{\frac{3}{2}}}\right]$$

Fig. 11. Lateral Stress Due to Finite Line Load Parallel to Wall

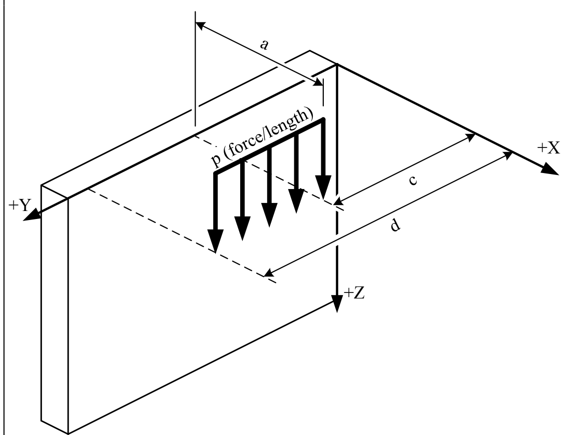

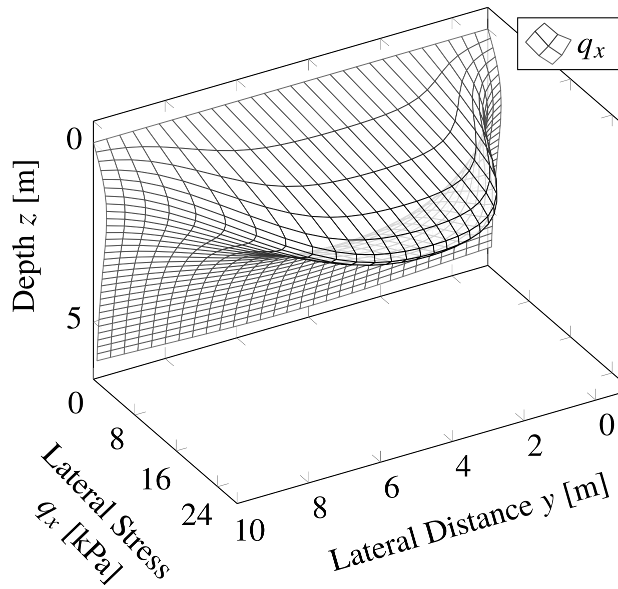

Sample stress distribution generated using the following parameters:
$\psi = 2$ $p = 70$ kN/m $\nu = 0.50$
$a = 2$ m $c = 1$ m $d = 8$ m

$$q_x(y,z) = \frac{\psi p}{2\pi a}\left[f_a - (1-2\nu) f_b\right]$$

$$f_a = \frac{a^3 z}{\left(a^2+z^2\right)^2}\left[\frac{(d-y)\left[3\left(a^2+z^2\right)+2(d-y)^2\right]}{\left[a^2+(d-y)^2+z^2\right]^{\frac{3}{2}}} - \frac{(c-y)\left[3\left(a^2+z^2\right)+2(c-y)^2\right]}{\left[a^2+(c-y)^2+z^2\right]^{\frac{3}{2}}}\right]$$

$$f_b = \tan^{-1}\left(\frac{d-y}{a}\right) - \tan^{-1}\left[\frac{z(d-y)}{a\sqrt{a^2+(d-y)^2+z^2}}\right] - \tan^{-1}\left(\frac{c-y}{a}\right) + \tan^{-1}\left[\frac{z(c-y)}{a\sqrt{a^2+(c-y)^2+z^2}}\right]$$

Fig. 12. Lateral Stress Due to Finite Line Load Perpendicular to Wall

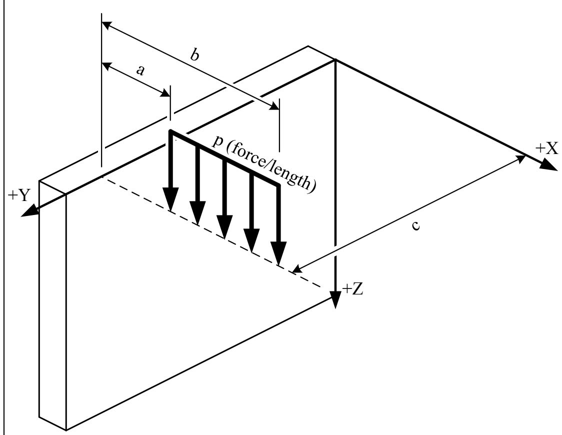

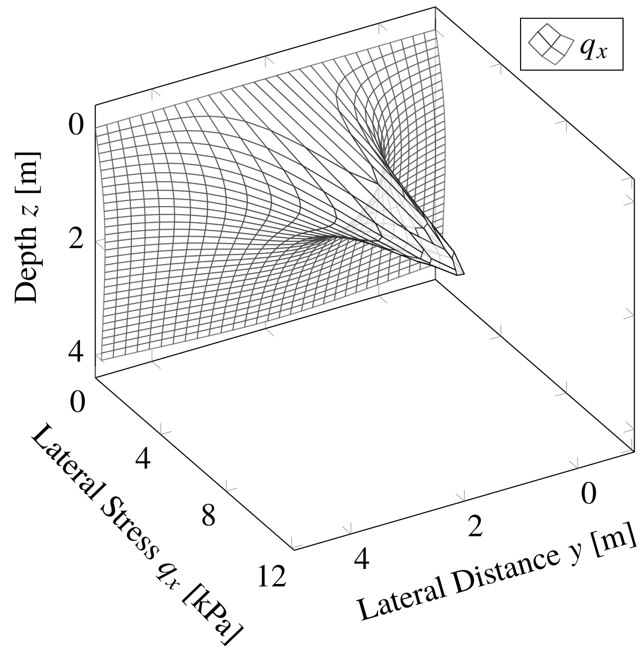

Sample stress distribution generated using the following parameters:
$\psi = 2$ $\quad p = 30$ kN/m $\quad \nu = 0.50$
$a = 0.5$ m $\quad b = 4$ m $\quad c = 2$ m

$$q_x(y,z) = \frac{\psi p}{2\pi}\left[f_a - (1-2\nu) f_b\right]$$

$$f_a = \frac{z}{(c-y)^2 + z^2}\left[b^3\left[b^2 + (c-y)^2 + z^2\right]^{-\frac{3}{2}} - a^3\left[a^2 + (c-y)^2 + z^2\right]^{-\frac{3}{2}}\right]$$

$$f_b = \begin{cases} \dfrac{\sqrt{b^2+z^2} - z}{bz} - \dfrac{\sqrt{a^2+z^2} - z}{az} & \text{if } y = c \\[2ex] \dfrac{1}{c-y}\left[\tan^{-1}\left[\dfrac{(c-y)(b-a)}{(c-y)^2 + ab}\right] - \tan^{-1}\left[\dfrac{bz}{(c-y)\sqrt{b^2 + (c-y)^2 + z^2}}\right]\right. \\ \qquad \left. + \tan^{-1}\left[\dfrac{az}{(c-y)\sqrt{a^2 + (c-y)^2 + z^2}}\right]\right] & \text{otherwise} \end{cases}$$

Fig. 13. Lateral Stress Due to Infinite Line Load Parallel to Wall

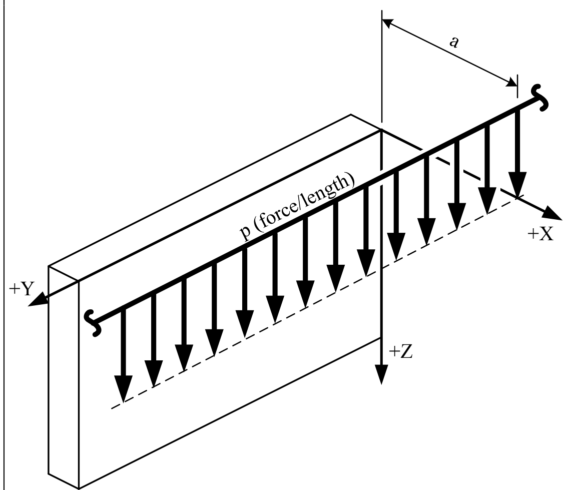

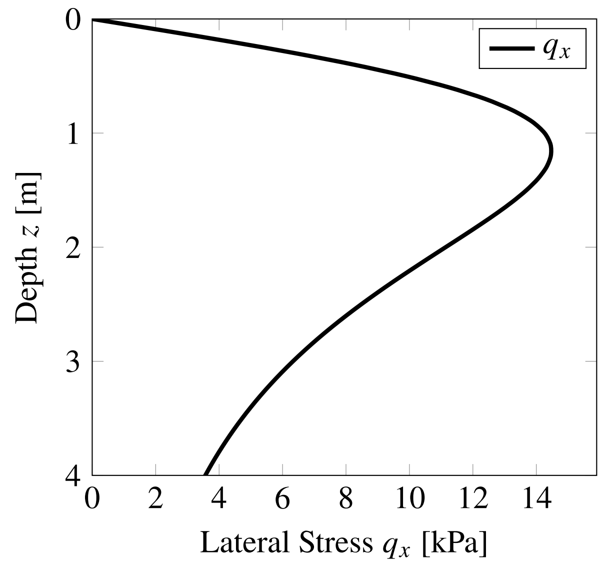

Sample stress distribution generated
using the following parameters:
$\psi = 2 \quad p = 70$ kN/m
$\nu = 0.50 \quad a = 2$ m

$$q_x(z) = \frac{\psi p}{2\pi a}\left[\frac{4a^3 z}{\left(a^2+z^2\right)^2} - (1-2\nu)\left[\pi - 2\tan^{-1}\left(\frac{z}{a}\right)\right]\right]$$

Fig. 14. Vertical Stress Due to Infinite Strip Load

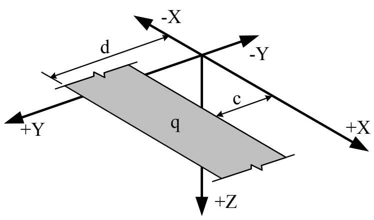

Sample stress distribution generated using the following parameters:

$q = 100$ kPa $c = -1.5$ m

$d = 1.5$ m $z = 2$ m

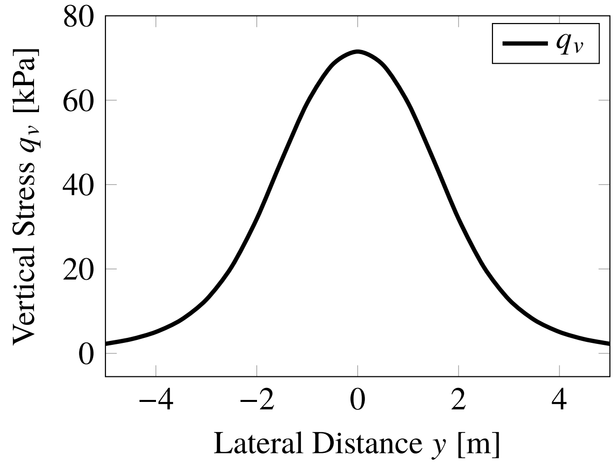

$$q_v(y) = \frac{q}{\pi}\left[\tan^{-1}\left(\frac{d-y}{z}\right) - \tan^{-1}\left(\frac{c-y}{z}\right) + z\left[\frac{d-y}{(d-y)^2+z^2} - \frac{c-y}{(c-y)^2+z^2}\right]\right]$$

Fig. 15. Vertical Stress Due to Finite Area Load

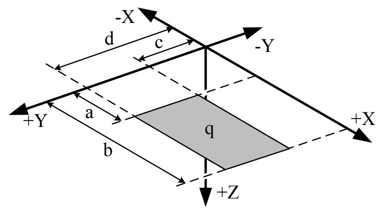

Sample stress distribution generated using the following parameters:
q = 100 kPa z = 1 m
a = −3 m b = 3 m
c = −2 m d = 2 m

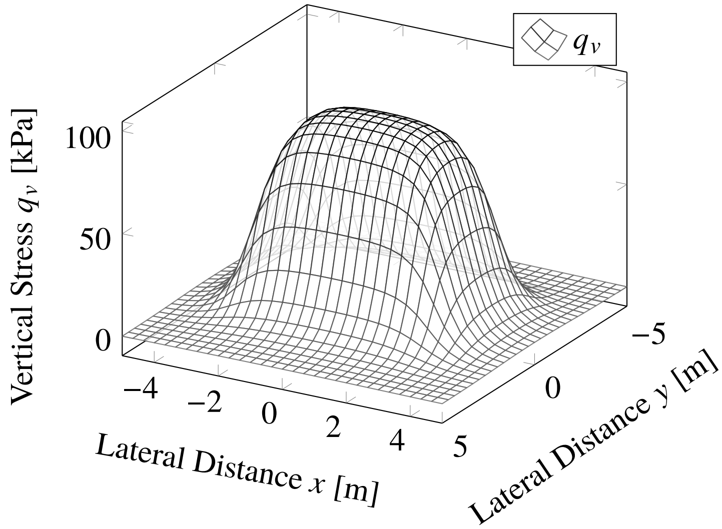

$$q_v(x, y) = \frac{q}{2\pi}\left[f(b, d) - f(a, d) - f(b, c) + f(a, c)\right]$$

$$f(\beta, \delta) = \frac{z(\beta - x)(\delta - y)\left[(\beta - x)^2 + (\delta - y)^2 + 2z^2\right]}{\left[(\beta - x)^2 + z^2\right]\left[(\delta - y)^2 + z^2\right]\sqrt{(\beta - x)^2 + (\delta - y)^2 + z^2}} + \tan^{-1}\left[\frac{(\beta - x)(\delta - y)}{z\sqrt{(\beta - x)^2 + (\delta - y)^2 + z^2}}\right]$$

Fig. 16. Lateral Stress Due to Infinite Strip Load Parallel to Wall

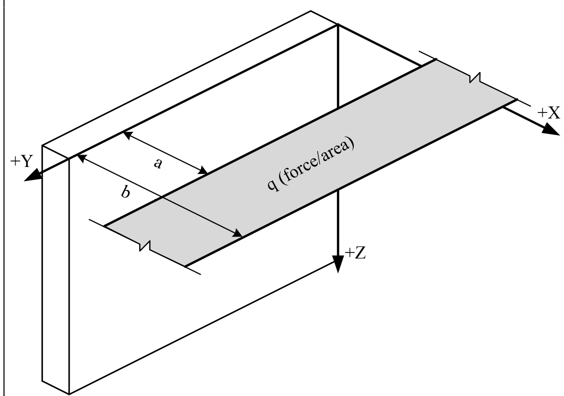

Sample stress distribution generated using the following parameters:
$\psi = 2$ $q = 100$ kPa
$a = 1$ m $b = 4$ m

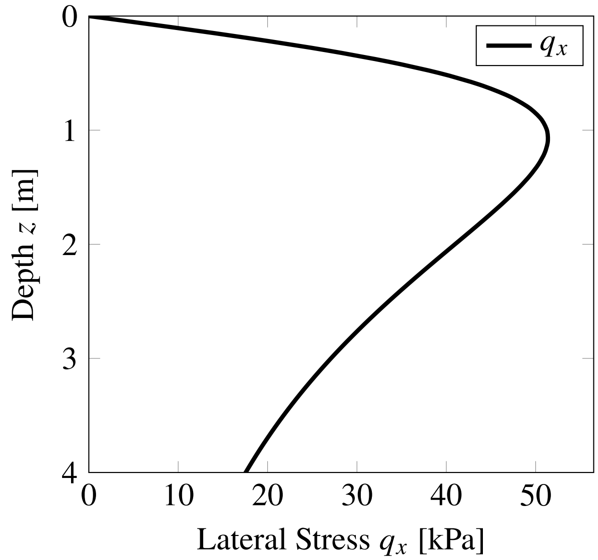

$$q_x(z) = \frac{\psi q}{\pi}\left[\frac{az}{a^2+z^2} - \frac{bz}{b^2+z^2} + \tan^{-1}\left(\frac{z(b-a)}{z^2+ab}\right)\right]$$

For the special case where $a = 0$, $q_x(z) = \begin{cases} \dfrac{\psi q}{2} \text{ if } z = 0 \\ \dfrac{q}{\pi}\left[\tan^{-1}\left(\dfrac{b}{z}\right) - \dfrac{bz}{b^2+z^2}\right] \text{ otherwise} \end{cases}$

Fig. 17. Lateral Stress Due to Finite Area Load

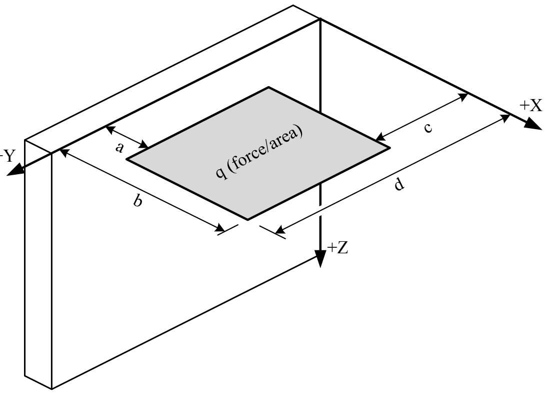

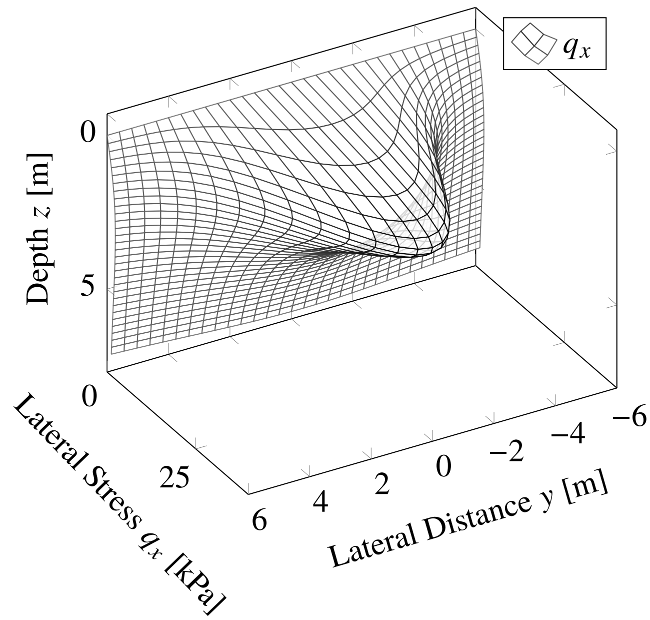

Sample stress distribution generated using the following parameters:

$\psi = 2 \quad q = 200$ kPa

$a = 2$ m $\quad b = 4$ m

$c = -2$ m $\quad d = 2$ m

$$q_x(y,z) = \frac{\psi q}{2\pi}\left[f(b,d) - f(b,c) - f(a,d) + f(a,c)\right]$$

$$f(\beta,\delta) = \tan^{-1}\left[\frac{\beta(\delta - y)}{z\sqrt{\beta^2 + (\delta - y)^2 + z^2}}\right] - \frac{\beta z(\delta - y)}{[\beta^2 + z^2]\sqrt{\beta^2 + (\delta - y)^2 + z^2}}$$

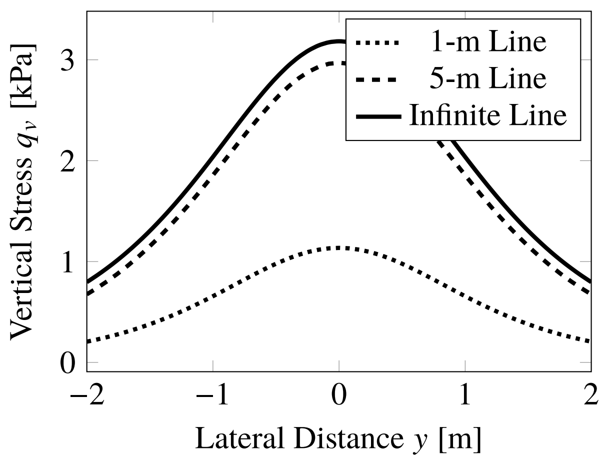

Fig. 18. Validation of Finite Line Load, Vertical Stress

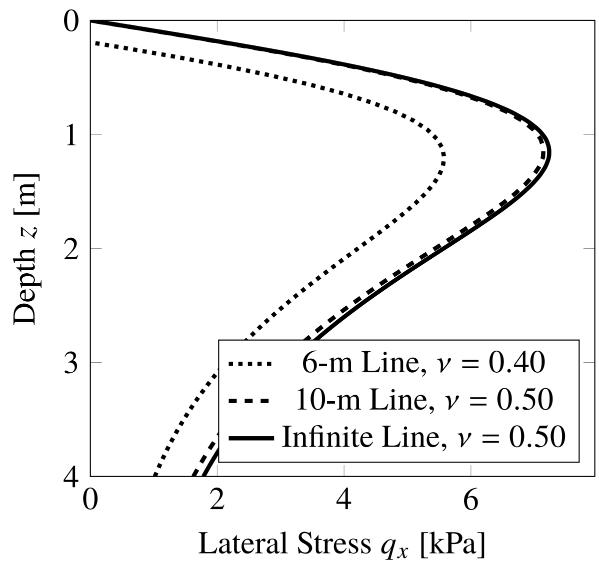

Fig. 19. Validation of Finite Line Load Parallel to Wall, Lateral Stress

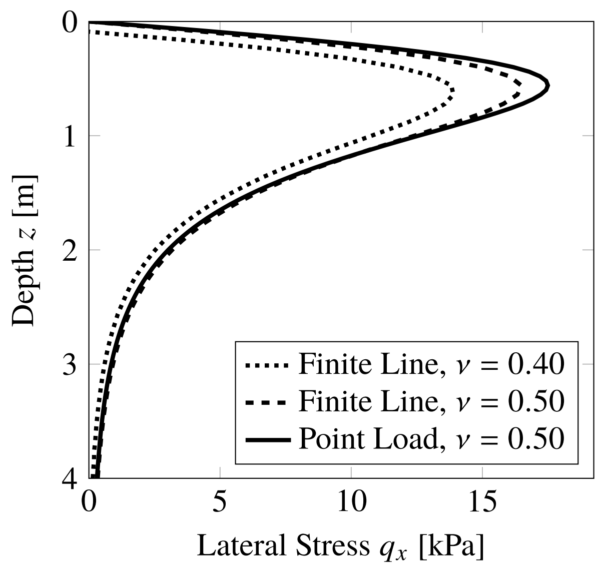

Fig. 20. Validation of Finite Line Load Perpendicular to Wall, Lateral Stress

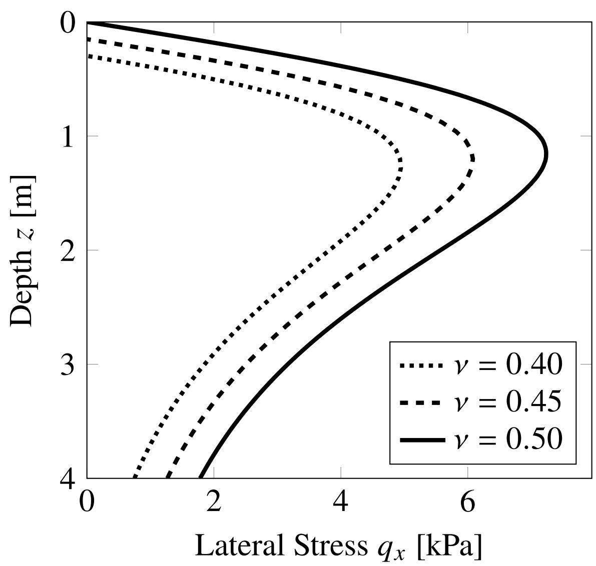

Fig. 21. Validation of Infinite Line Load Parallel to Wall, Lateral Stress

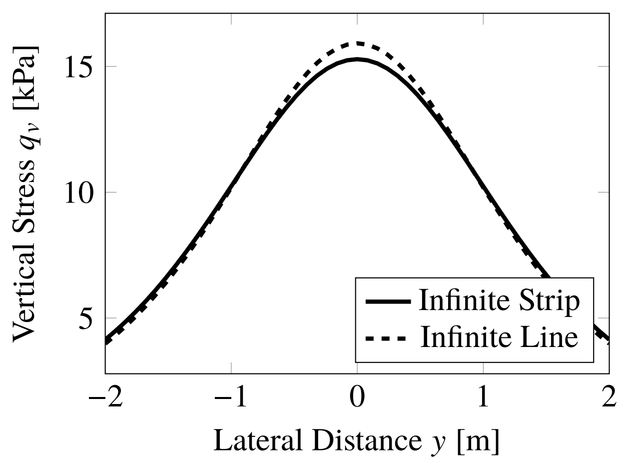

Fig. 22. Validation of Infinite Strip Load, Vertical Stress

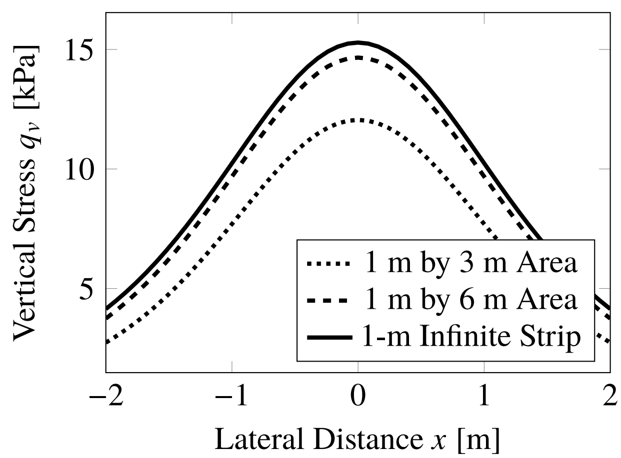

Fig. 23. Validation of Finite Area Load, Vertical Stress

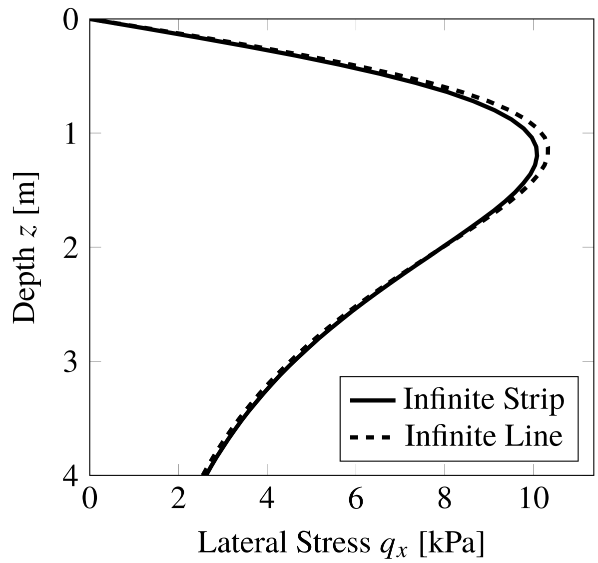

Fig. 24. Validation of Infinite Strip Load, Lateral Stress

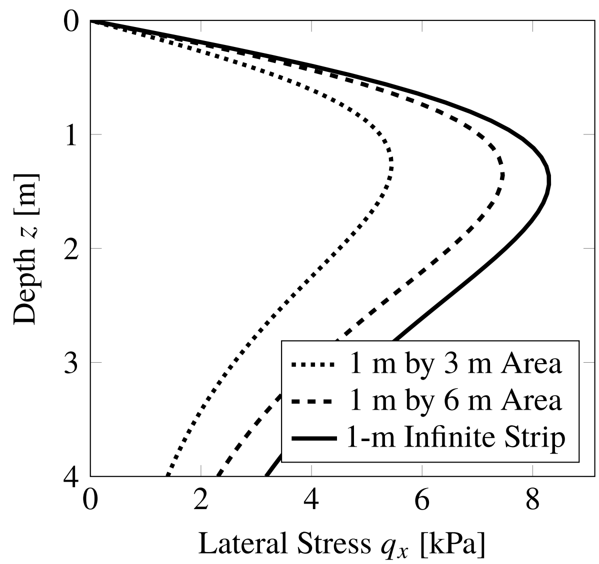

Fig. 25. Validation of Finite Area Load, Lateral Stress